TEM and STEM Image Simulation

Winter School on High Resolution Electron Microscopy
Held at the
John M. Cowley Center for High Resolution Electron Microscopy
January 7 - 11, 2019

Pierre Stadelmann
JEMS-SAAS
CH-3906 Saas-Fee
Switzerland

May 25, 2019

TEM: reminder

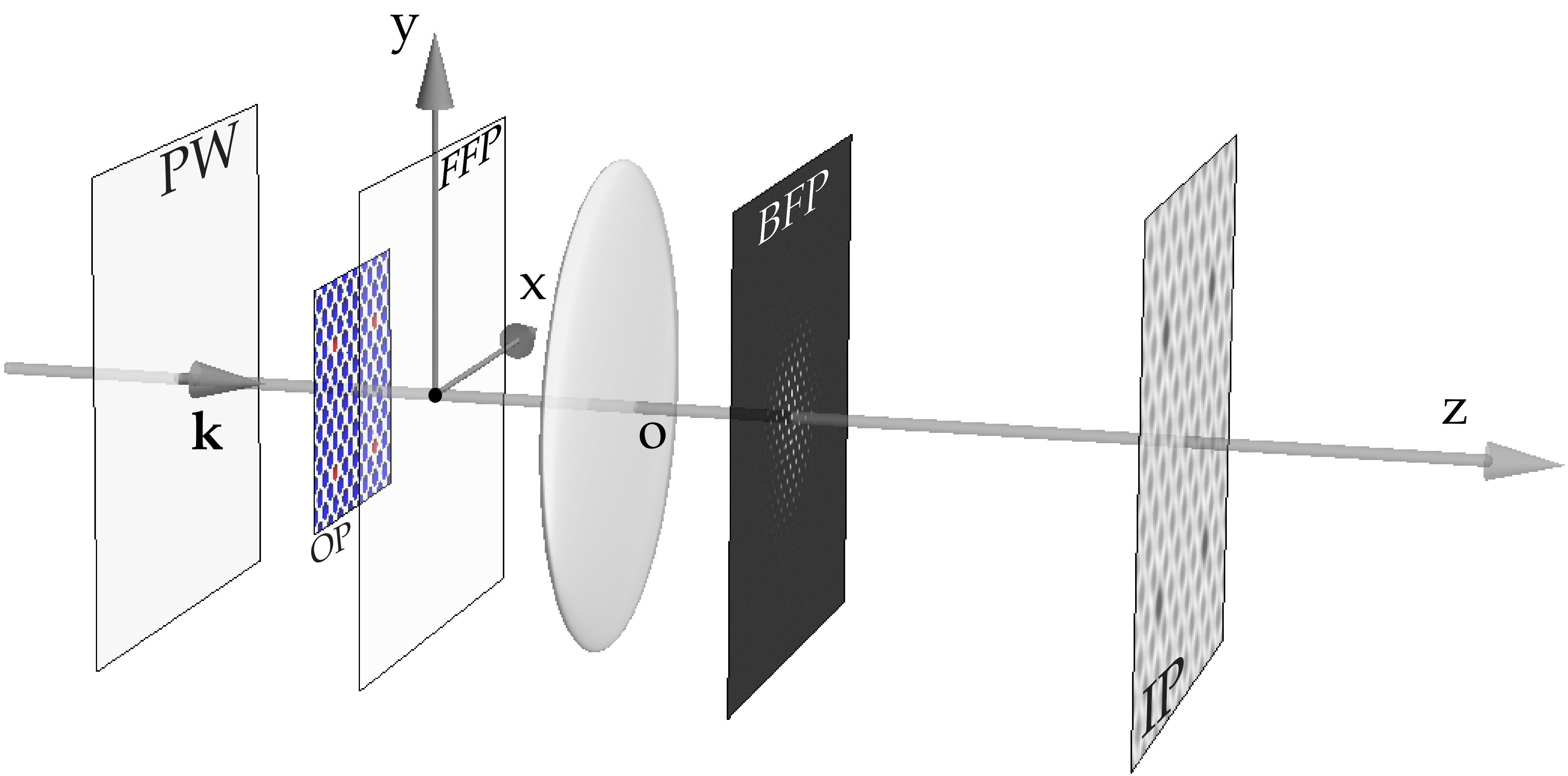

TEM modelling steps: incident wave (PW), crystal (OP), electron-matter interaction, Fraunhofer approximation, image formation (Abbe theory), ...

Image wave-function: $|\Psi_i>$

$$|\chi> \implies \text{incident wave-function}$$

$$|\Psi_i> = \underbrace{\sum^{q'} < \rho|q'>}_{\text{Fourier synthesis}} \underbrace{\sum^{q} < q'|T(q',q)|q>}_{\text{Objective lens transfer}} \underbrace{< q|\widehat{U}(z,0)|\chi>}_{\text{Fourier transform}}$$

- $\longrightarrow$**Dynamical calculations: how good**?
- Optical system.
- Aberrations.
- TEM transfer function & STEM: optical transfer function.
- Comparison HRTEM - HRSTEM.

$| < q|\widehat{U}(z,0)|\chi > |^2$

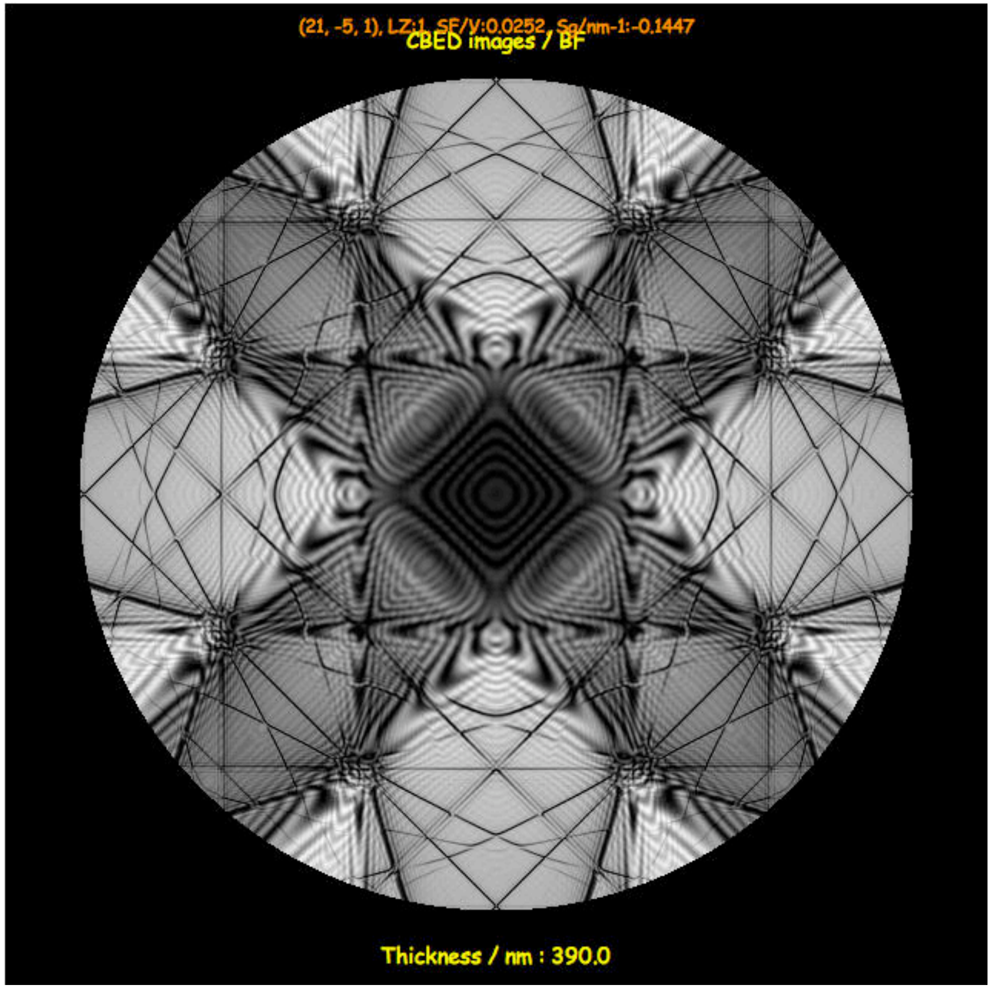

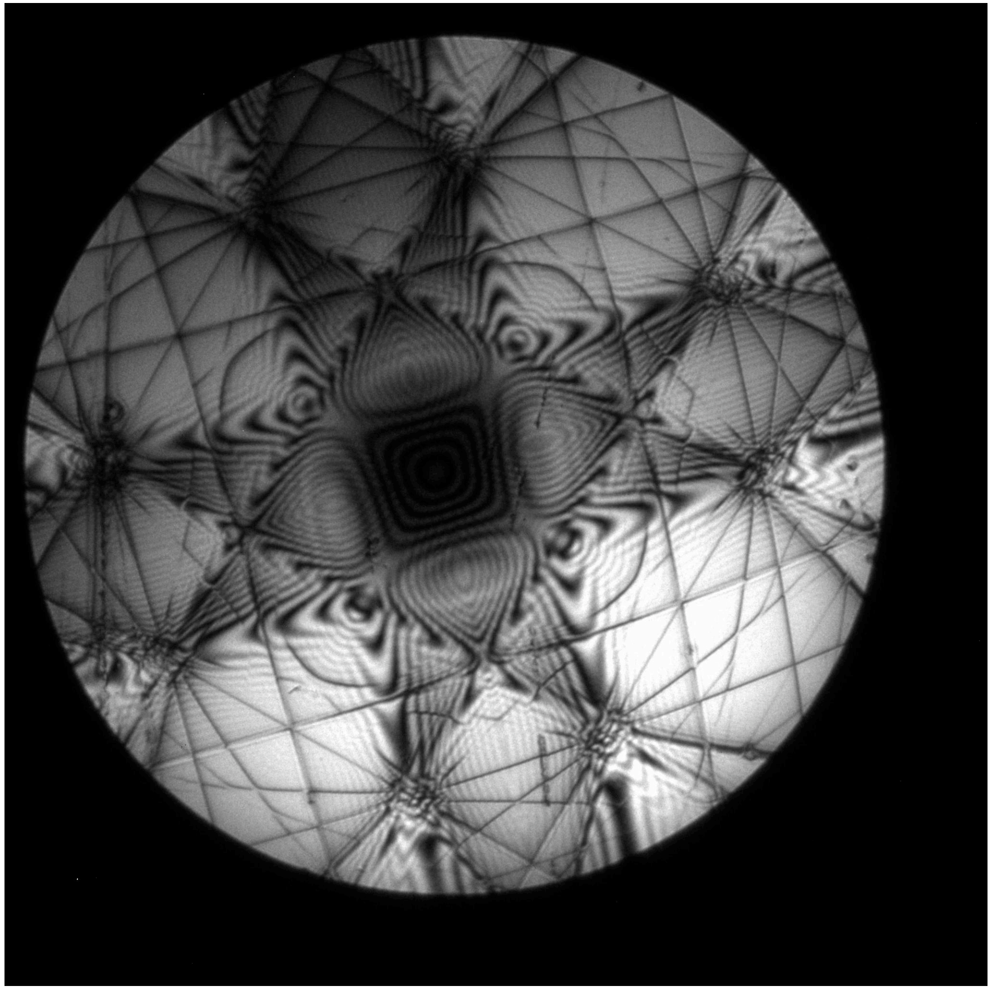

LACBED Si [001]: simulation.

LACBED Si [001]: experimental (Web site EM centre - Monash university, J. Etheridge).

Note that the experimental LACBED pattern is blurred (inelastic scattering and/or MTF of CCD camera).

- Dynamical calculations: how good?
- $\longrightarrow$**Optical system**.
- Aberrations.
- TEM transfer function & STEM: optical transfer function.
- Comparison HRTEM - HRSTEM.

Optical system: $\sum^q < q'|T(q',q)|q >$

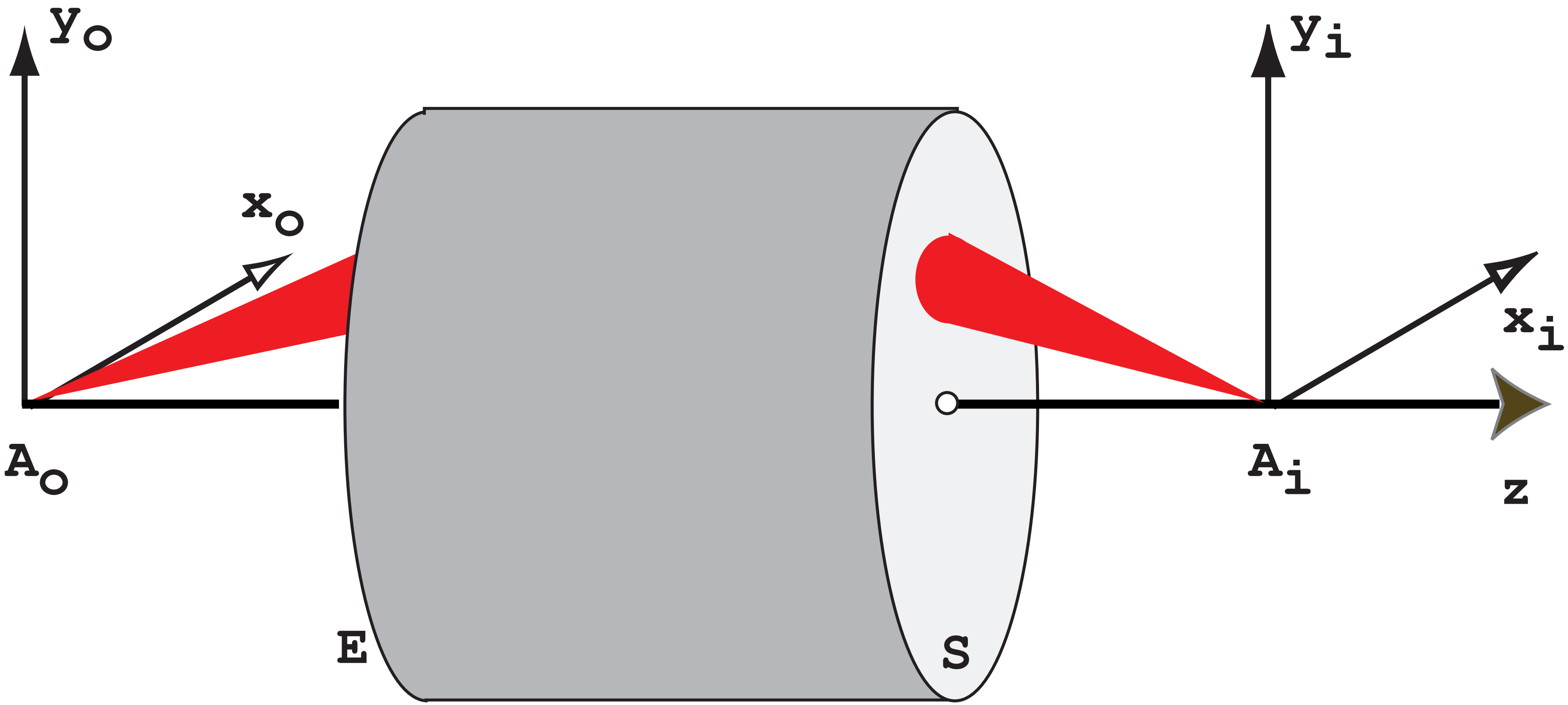

An optical system produces the image A_i of a point source object A_o. A_o and A_i are said to be conjugate. A_i is not a point but spot, the Airy disk, since **any optical system is diffraction limited**. This limitation is introduced by the entrance and exit pupils of the optical system.

Transfer function

An optical system as a "black box" that gives an image wave-function $\Psi_i(\vec{x})$ of an object wave-function $\Psi_o(\vec{x})$:

$$\Psi_i(\vec{x}) = S\{\Psi_o(\vec{x})\}$$

It must have 2 properties to be described by a point spread function $PSF(\vec{x})$ (or a transfer function $\widetilde{T}(\vec{q})$).

1. Linearity.
2. Space invariance.

Transfer function: property 1

Linearity

$$\begin{aligned} S\{a_1\Psi_o^1(\vec{x}) + a_2\Psi_o^2(\vec{x})\} &= a_1 S\{\Psi_o^1(\vec{x})\} + a_2 S\{\Psi_o^2(\vec{x})\} \\ S\{a_1\Psi_o^1(\vec{x}) + a_2\Psi_o^2(\vec{x})\} &= a_1\Psi_i^1(\vec{x}) + a_2\Psi_i^2(\vec{x}) \end{aligned}$$

Linearity allows to decompose the object wave-function in ∞ sum of point sources:

$$\Psi_o(\vec{x}) = \int_{-\infty}^{\infty} \Psi_o(\vec{\zeta})\delta(\vec{x}-\vec{\zeta})\mathrm{d}\vec{\zeta}$$

Image wave-function $\Psi_i(\vec{x})$:

$$\Psi_i(\vec{x}) = S\left\{\int_{-\infty}^{\infty} \Psi_o(\vec{\zeta})\delta(\vec{x}-\vec{\zeta})\mathrm{d}\vec{\zeta}\right\} = \int_{-\infty}^{\infty} \Psi_o(\vec{\zeta}) S\{\delta(\vec{x}-\vec{\zeta})\}\mathrm{d}\vec{\zeta}$$

$$\Psi_i(\vec{x}) = \int_{-\infty}^{\infty} \Psi_o(\vec{\zeta}) T(\vec{x};\vec{\zeta})\mathrm{d}\vec{\zeta}$$

where $T(\vec{x};\vec{\zeta}) = S\{\delta(\vec{x}-\vec{\zeta})\}$: **Impulse Response** of optical system S.

Transfer function: property 2

Space invariance

Space invariance is realised when the image of a point source is independent of its position in the object plane, i.e. when the point source moves in the object plane its image moves similarly in the image plane without changing form and intensity.

$$T(\vec{x};\vec{\zeta}) = T(\vec{x}-\vec{\zeta})$$

$$\Psi_i(\vec{x}) = \int_{-\infty}^{\infty} \Psi_o(\vec{\zeta})\,T(\vec{x}-\vec{\zeta})\mathrm{d}\vec{\zeta} = \Psi_o(\vec{x}) \otimes T(\vec{x})$$

Convolution integral spreads object information, degrades performance of optical system.

In Fourier space:

$$\widetilde{\Psi}_i(\vec{q}) = \widetilde{\Psi}_o(\vec{q})\,\widetilde{T}(\vec{q})$$

$\widetilde{T}(\vec{q})$: transfer function of optical system.

- Dynamical calculations: how good?
- Optical system.
- $\longrightarrow$**Aberrations**.
- TEM transfer function & STEM: optical transfer function.
- Comparison HRTEM - HRSTEM.

Pupils

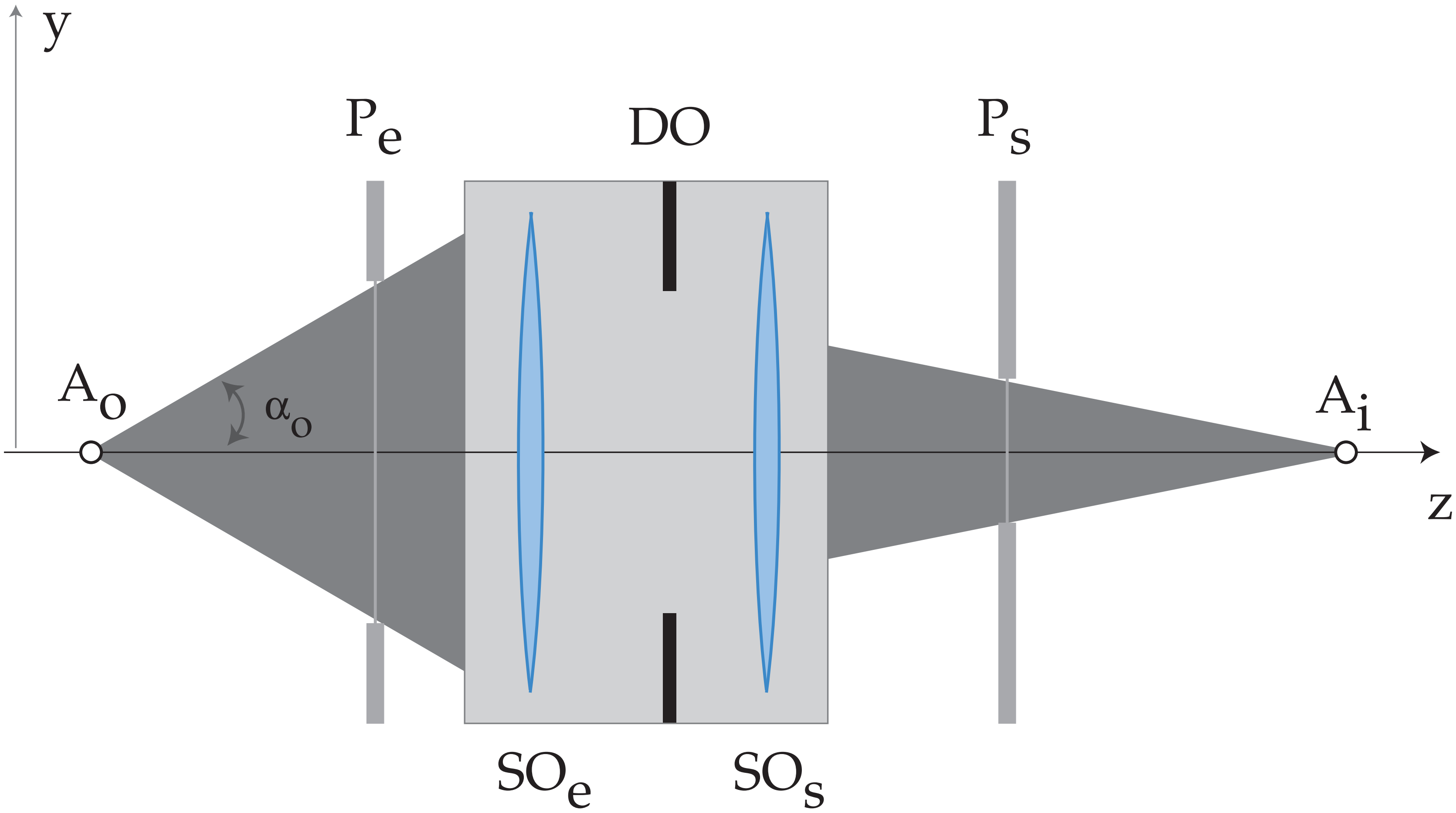

Any optical system can be characterised by an entrance pupil P_e and an exit pupil P_s. The pupils are the image of the opening aperture *DO* by the entrance and exit optical subsystems SO_e and SO_s. The portion of the object wave-function accepted by the optical system is limited by P_e, while SO_s limits the extend of the image wave-function. For a **perfect** optical system, the image of a point source will be an Airy disk.

Airy disks and Rayleigh resolution criterion

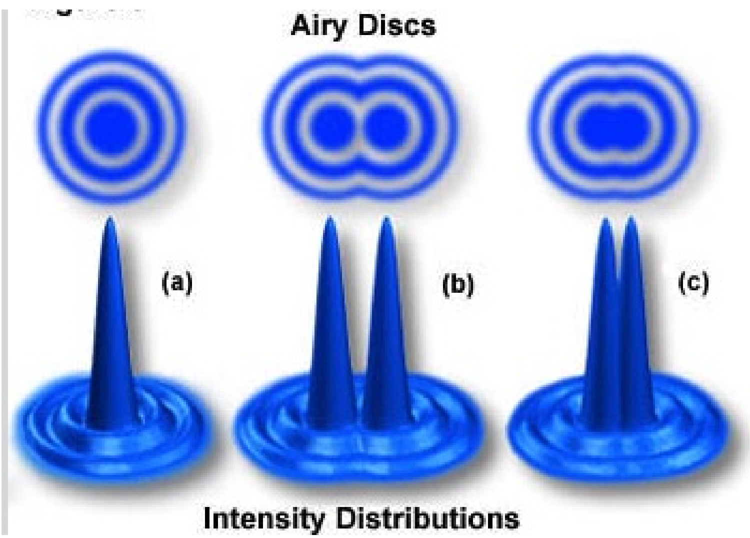

Airy disks.

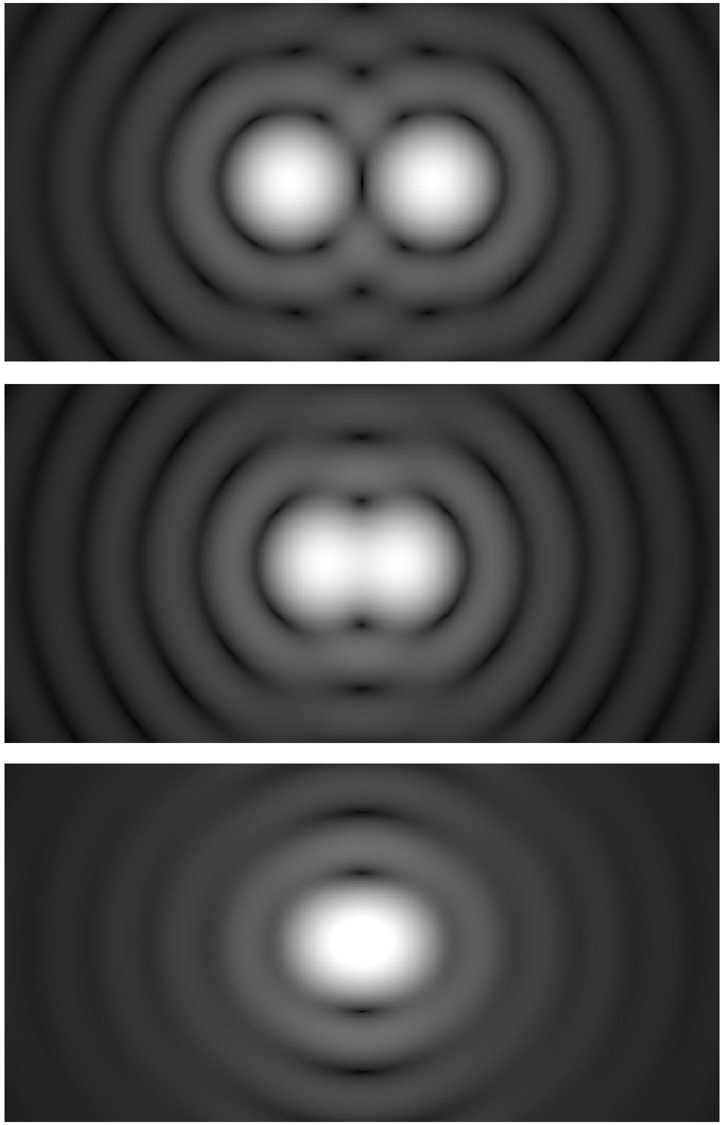

Airy disks near Rayleigh resolution criterion.

Some light rays emitted by object point A_o do not reach the image at point A_i.

Position of $A_i \longrightarrow$ intersection of the reference light ray (non deviated) and the image plane.

The image of a point source is a **spot** whose shape and intensity depend of the quality of the optical system.

Two types of aberrations:

1. Monochromatic.
2. Chromatic (λ dependent).

Monochromatic aberrations

In order to evaluate the monochromatic aberrations one must define a function characteristic of the optical system.

This function will depend on:

1. The selected reference planes.
2. The optical path followed by the light ray.

The important feature is the optical path length (OPL).

$$OPL(P_1P_2) = \int_{P_1}^{P_2} n(\overrightarrow{r})\, ds$$

1. OPL is measured in meters ($n(\vec{r}) = \frac{c}{v(\vec{r})}$ has no unit).
2. OPL is proportional to the time spent by the light ray to travel from P_1 to P_2.
3. Surface of constant OPL $\longrightarrow$ wavefront (surface of constant travel time).
4. OPL is measured from the entrance pupil P_E to the exit pupil P_S.

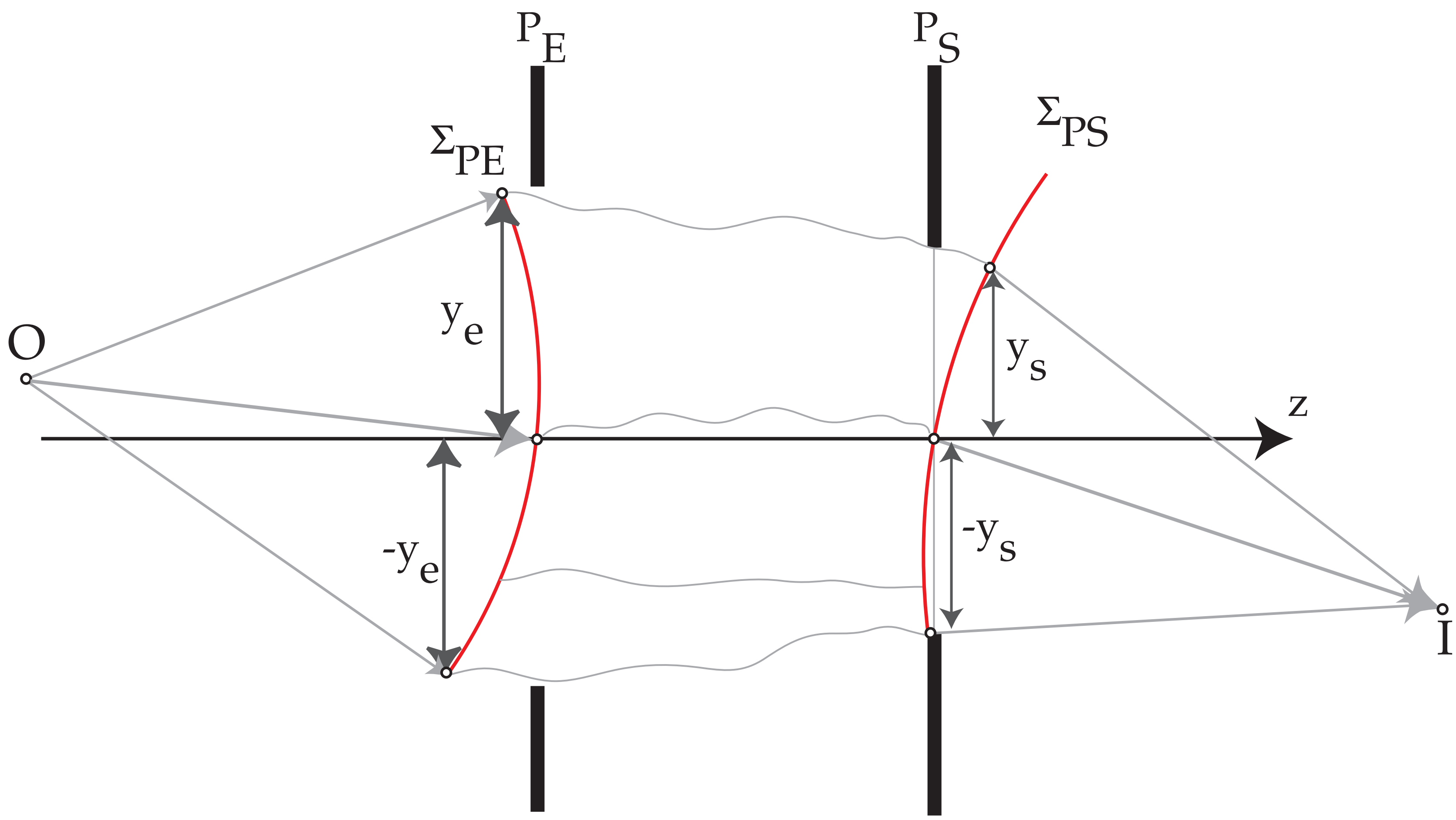

- Before P_E the reference wavefront Σ_{PE} is spherical (point source at O).
- After P_S the reference wavefront Σ_{PS} is spherical (converges towards I).

For a perfect optical system, both the entrance Σ_{PE} and exit Σ_{PS} wavefronts are spherical. The Optical Path Length form O to I is independent of the path.

Optical Path Difference: OPD

The OPD measure the deviation of a wavefront from a perfect spherical wavefront (vacuum or homogenous medium).
At the exit pupil P_S, the spherical wavefront converging towards **I** defines the reference wavefront.

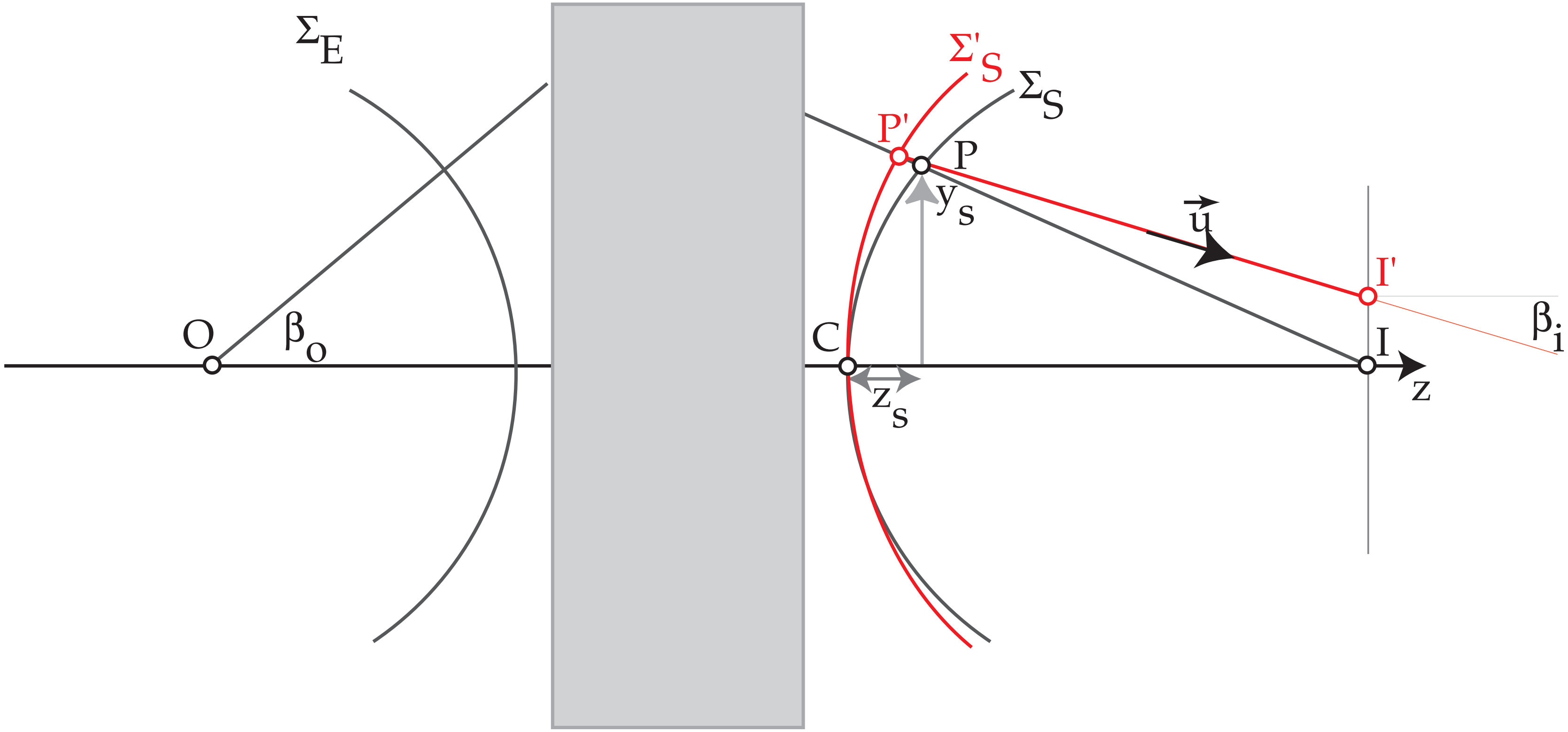

In the presence of aberrations the wavefront Σ_S' is no more spherical. The Optical Path Difference, $\overline{P'P}$ (distance between the deformed Σ_S' and spherical wavefront Σ_S) introduces the phase shift:

$$\delta\phi = e^{2\pi\imath\frac{OPD(x_S,y_S)}{\lambda}}$$

Transverse geometric aberrations: $\vec{\epsilon}$

The transverse geometric aberrations are proportional to $\frac{d}{d\theta}$ wavefront aberrations[1]:

$$\epsilon_x = -\frac{f}{n_i}\frac{\partial W}{\partial x_s}$$
$$\epsilon_y = -\frac{f}{n_i}\frac{\partial W}{\partial y_s}$$

f focal length.

The OPD's introduced by all the aberrations of the imaging system are collected in a function $\chi(\vec{q})$ and the phase shift is[2]:

$$\widetilde{T}(\vec{q}) = e^{-\imath\chi(\vec{q})}$$

$\widetilde{T}(\vec{q})$ has been first employed by Abbe in his description of image formation (1866).

[1] $P(x_s, y_s)$ on the spherical reference wavefront can be characterised by the radial angle θ.

[2] The angle θ corresponds (through Bragg law) to a spatial frequency $\vec{q}$, i.e. a distance in the back focal plane.

OPD: spherical aberration

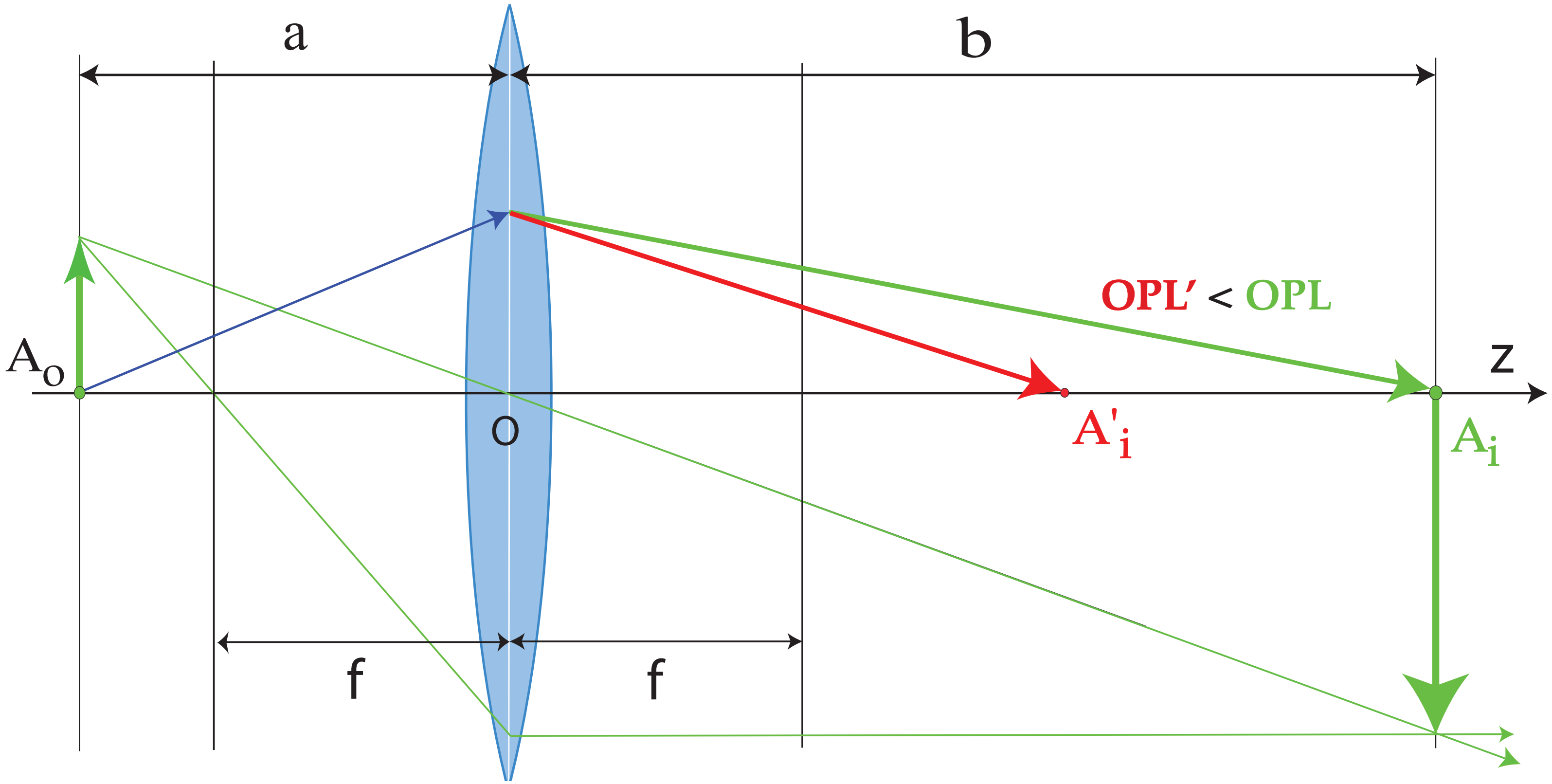

In presence of spherical aberration, the optical path length (OPL') form A_o to A'_i is smaller than OPL from A_o to A_i. The wavefront at A'_i is out-of-phase by[3]:

$$e^{-2\pi i \frac{C_s \lambda^3 (\vec{q}.\vec{q})^2}{4}}$$

[3]With our plane wave choice $e^{2\pi \imath \vec{q}.\vec{r}}$.

OPD: underfocus

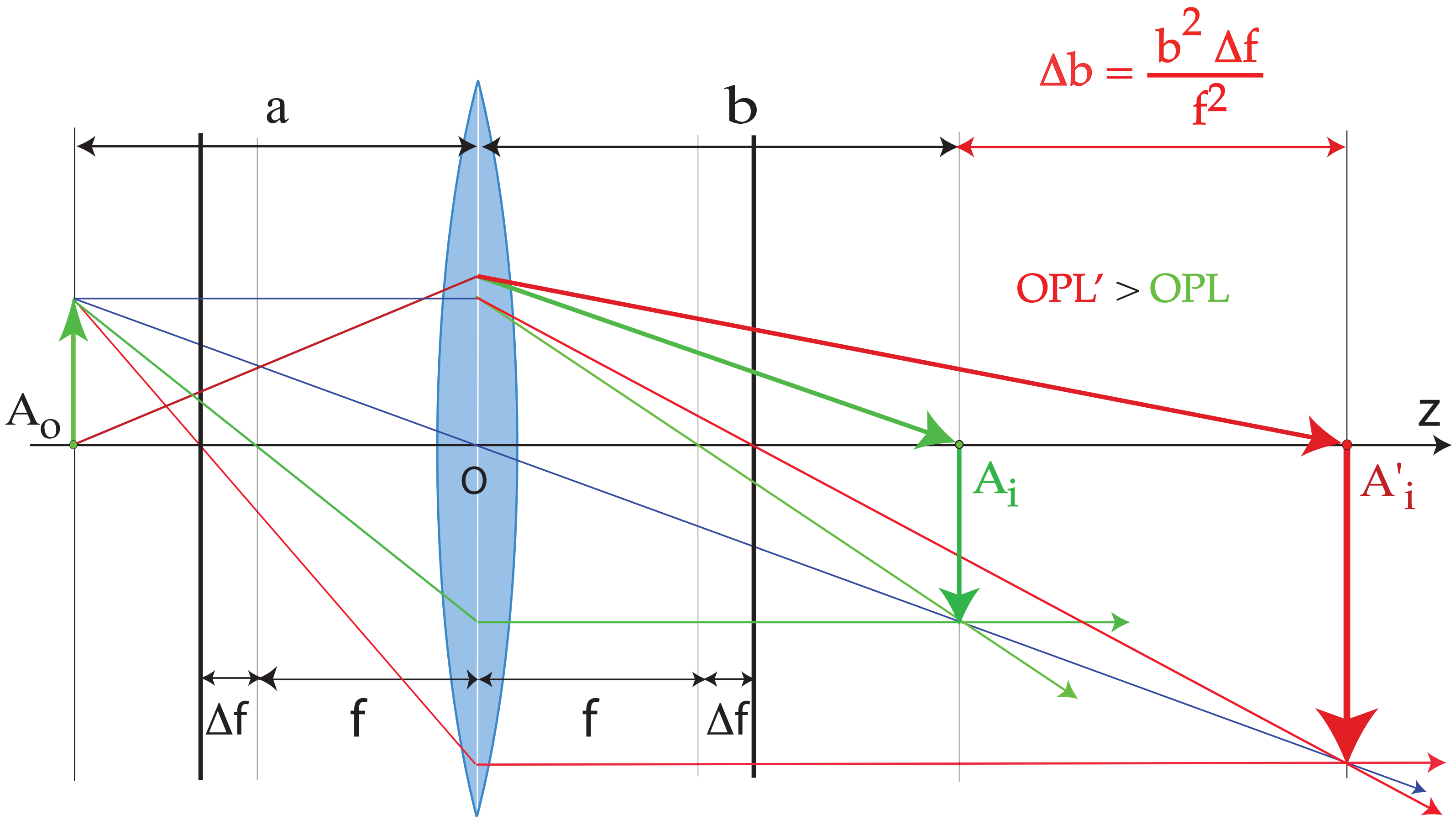

Underfocus weakens the objective lens, i.e. increases **f**. As a consequence the OPL from A_o to A'_i is larger:

$$e^{2\pi i \frac{\Delta f \lambda (\vec{q}\cdot\vec{q})}{2}}$$

OPD: eccentricity

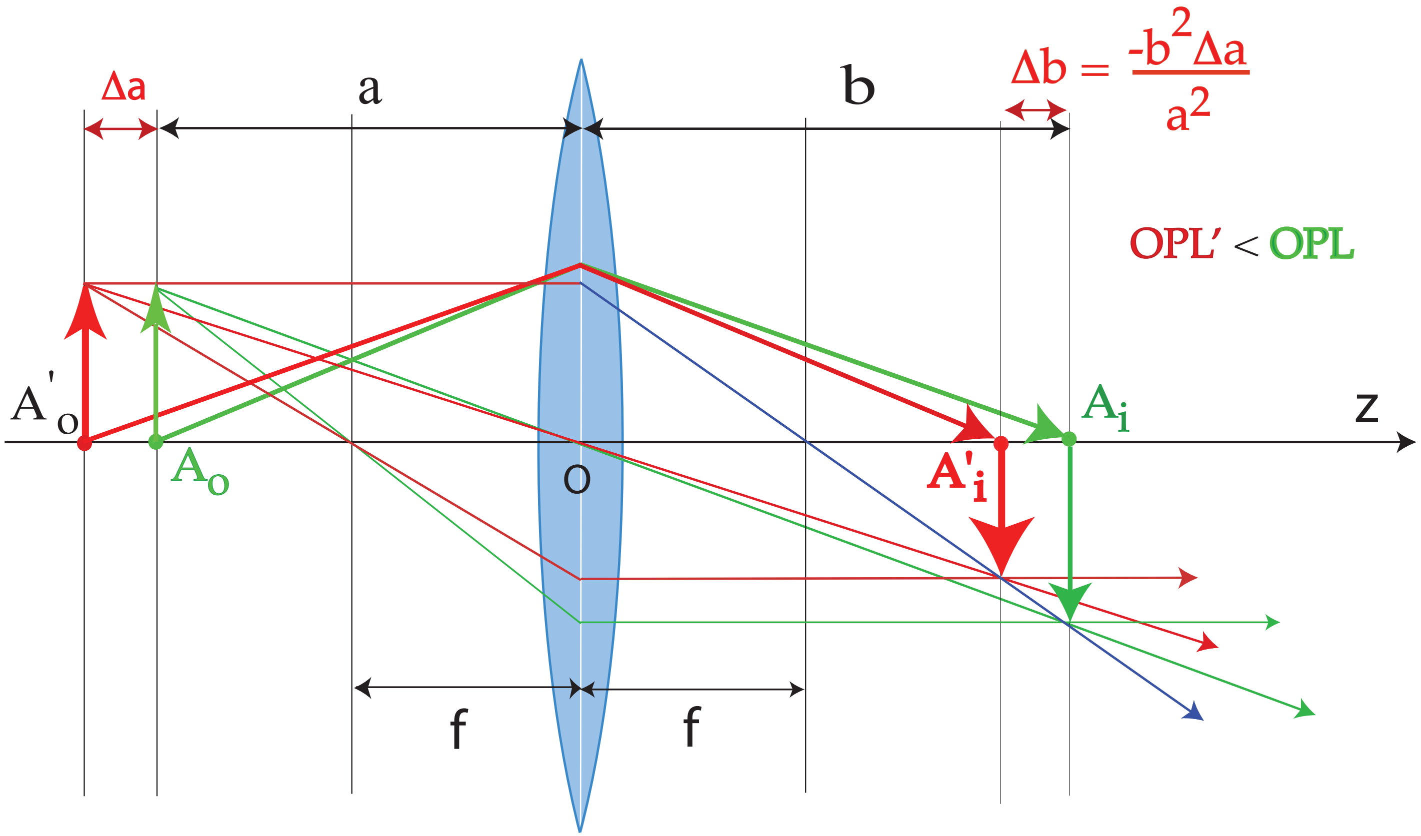

On the contrary keeping **f** constant and moving the object by Δa decreases the OPL.

$$\widetilde{T}(\vec{q}) = e^{-\imath\chi(\vec{q})} = \cos(\chi(\vec{q})) - \imath \underbrace{\sin(\chi(\vec{q}))}_{\text{PCTF}}$$

Phase Contrast Transfer Function

$$\chi(\vec{q}) = \pi \left[-W_{20}\,\lambda\,(\vec{q}.\vec{q}) + W_{40}\frac{\lambda^3\,(\vec{q}.\vec{q})^2}{2} + ... \right]$$

Where:

- W_{20} : defocus (z)
- W_{40}: spherical aberration (C_s)

At present TEM and STEM aberration correctors only correct axial aberrations, i.e. aberrations that affect images of point sources located on the optical axis.

Wavefront aberrations to 6^{th} order (cartesian coordinates)

$\{z, \pi\left(u^2+v^2\right)\lambda\}$ *(defocus)*

$\{W(1,1), 2\pi(u\cos(\phi(1,1)) + v\sin(\phi(1,1)))\}$

$\{W(2,2), \pi\lambda((u-v)(u+v)\cos(2\phi(2,2)) + 2uv\sin(2\phi(2,2)))\}$

$\left\{W(3,1), \frac{2}{3}\pi\left(u^2+v^2\right)\lambda^2(u\cos(\phi(3,1)) + v\sin(\phi(3,1)))\right\}$

$\left\{W(3,3), \frac{2}{3}\pi\lambda^2\left(u\left(u^2-3v^2\right)\cos(3\phi(3,3)) - v\left(v^2-3u^2\right)\sin(3\phi(3,3))\right)\right\}$

$\left\{W(4,0), \frac{1}{2}\pi\left(u^2+v^2\right)^2\lambda^3\right\}$ *(3^{rd} order spherical aberration or C_3)*

$\left\{W(4,2), \frac{1}{2}\pi\left(u^2+v^2\right)\lambda^3((u-v)(u+v)\cos(2\phi(4,2)) + 2uv\sin(2\phi(4,2)))\right\}$

$\left\{W(4,4), \frac{1}{2}\pi\lambda^3\left(\left(u^4-6v^2u^2+v^4\right)\cos(4\phi(4,4)) + 4u(u-v)v(u+v)\sin(4\phi(4,4))\right)\right\}$

$\left\{W(5,1), \frac{2}{5}\pi\left(u^2+v^2\right)^2\lambda^4(u\cos(\phi(5,1)) + v\sin(\phi(5,1)))\right\}$

$\left\{W(5,3), \frac{2}{5}\pi\left(u^2+v^2\right)\lambda^4\left(u\left(u^2-3v^2\right)\cos(3\phi(5,3)) - v\left(v^2-3u^2\right)\sin(3\phi(5,3))\right)\right\}$

$\left\{W(5,5), \frac{2}{5}\pi\lambda^4\left(u\left(u^4-10v^2u^2+5v^4\right)\cos(5\phi(5,5)) + v\left(5u^4-10v^2u^2+v^4\right)\sin(5\phi(5,5))\right)\right\}$

$\left\{W(6,0), \frac{1}{3}\pi\left(u^2+v^2\right)^3\lambda^5\right\}$ *(5^{th} order spherical aberration or C_5)*

$\left\{W(6,2), \frac{1}{3}\pi\left(u^2+v^2\right)^2\lambda^5((u-v)(u+v)\cos(2\phi(6,2)) + 2uv\sin(2\phi(6,2)))\right\}$

$\left\{W(6,4), \frac{1}{3}\pi\lambda^5\left(\left(u^6-5v^2u^4-5v^4u^2+v^6\right)\cos(4\phi(6,4)) + 4uv\left(u^4-v^4\right)\sin(4\phi(6,4))\right)\right\}$

$\left\{W(6,6), \frac{1}{3}\pi\lambda^5\left(\left(u^6-15v^2u^4+15v^4u^2-v^6\right)\cos(6\phi(6,6)) + 2uv\left(3u^4-10v^2u^2+3v^4\right)\sin(6\phi(6\right.\right.$

jems describes wavefront aberrations to order 8. And provides a dictionary of equivalent notation:

Wave-front aberrations to order 8

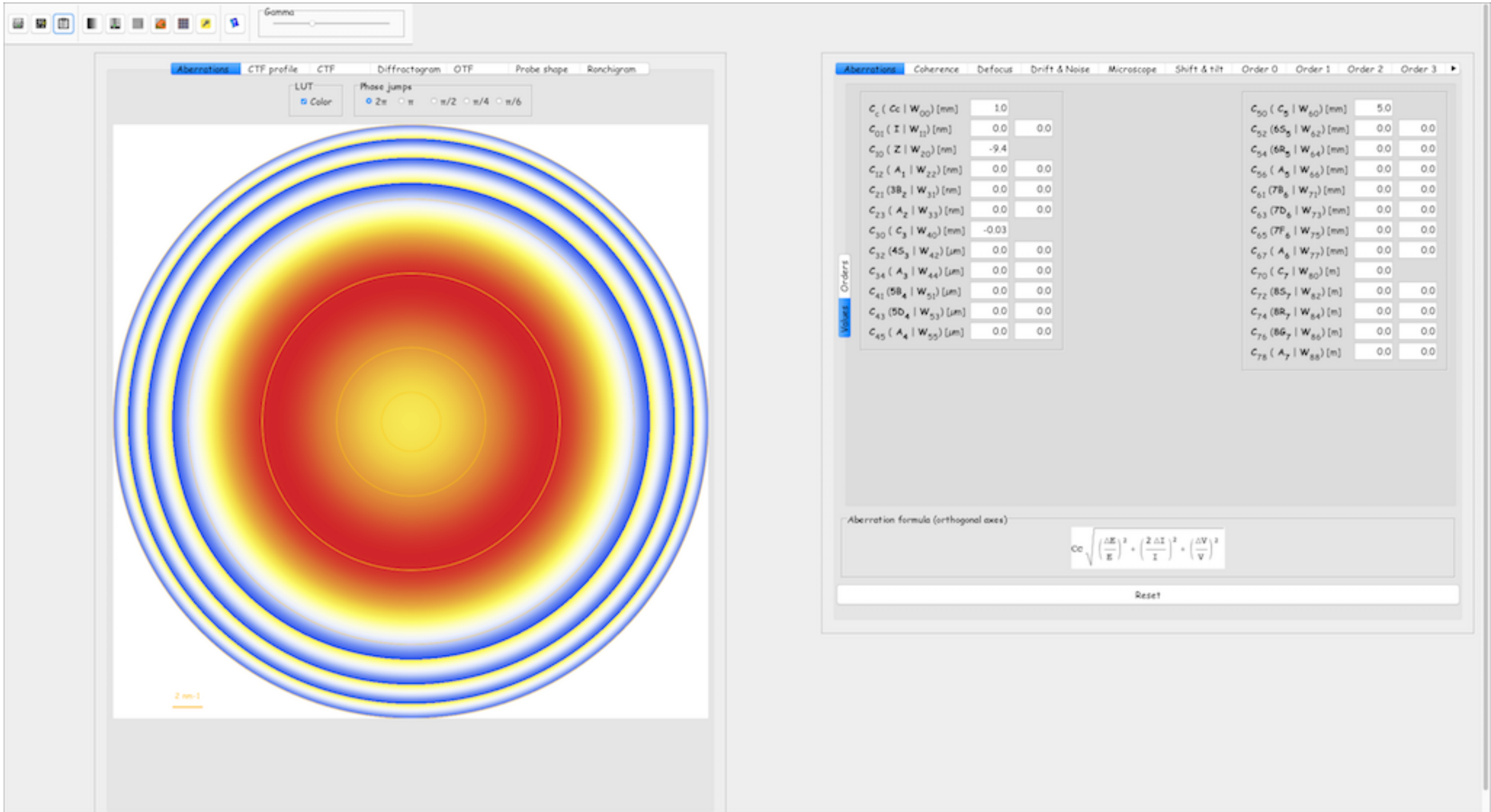

Wavefront aberrations up to order 8 can be introduced in HRTEM image formation and HRSTEM probe formation.

Aberrations dictionary (order 8)

C_c (Cc | W_{00}) [mm]	1.0	
C_{01} (I | W_{11}) [nm]	0.0	0.0
C_{10} (Z | W_{20}) [nm]	-9.4	
C_{12} (A_1 | W_{22}) [nm]	0.0	0.0
C_{21} ($3B_2$ | W_{31}) [nm]	0.0	0.0
C_{23} (A_2 | W_{33}) [nm]	0.0	0.0
C_{30} (C_3 | W_{40}) [mm]	-0.03	
C_{32} ($4S_3$ | W_{42}) [µm]	0.0	0.0
C_{34} (A_3 | W_{44}) [µm]	0.0	0.0
C_{41} ($5B_4$ | W_{51}) [µm]	0.0	0.0
C_{43} ($5D_4$ | W_{53}) [µm]	0.0	0.0
C_{45} (A_4 | W_{55}) [µm]	0.0	0.0

C_{50} (C_5 | W_{60}) [mm]	5.0	
C_{52} ($6S_5$ | W_{62}) [mm]	0.0	0.0
C_{54} ($6R_5$ | W_{64}) [mm]	0.0	0.0
C_{56} (A_5 | W_{66}) [mm]	0.0	0.0
C_{61} ($7B_6$ | W_{71}) [mm]	0.0	0.0
C_{63} ($7D_6$ | W_{73}) [mm]	0.0	0.0
C_{65} ($7F_6$ | W_{75}) [mm]	0.0	0.0
C_{67} (A_6 | W_{77}) [mm]	0.0	0.0
C_{70} (C_7 | W_{80}) [m]	0.0	
C_{72} ($8S_7$ | W_{82}) [m]	0.0	0.0
C_{74} ($8R_7$ | W_{84}) [m]	0.0	0.0
C_{76} ($8G_7$ | W_{86}) [m]	0.0	0.0

Notation

7th order chapelet aberration (C76::W86::8G7)

Formula

$$\frac{1}{8}\lambda^7\left(\left(u^8-14u^6v^2+14u^2v^6-v^8\right)\text{Cos}[6\phi_{86}]+2uv\left(3u^6-7u^4v^2-7u^2v^4+3v^6\right)\text{Sin}[6\phi_{86}]\right)$$

Equivalent aberration notation (Krivanek, Rose/Haider, wave-front aberrations).

- Dynamical calculations: how good?
- Optical system.
- Aberrations.
- $\longrightarrow$**HRTEM Transfer Function & $\longrightarrow$HRSTEM: Optical Transfer Function**.
- Comparison HRTEM - HRSTEM.

HRTEM

coherent or partially coherent image formation process with coherent or partially coherent incident wave.

TEM ($\widetilde{T}(\vec{q})$: Transfer Function):

$$\begin{aligned}\widetilde{\Psi}_i(\vec{q}) &= \widetilde{\Psi}_o(\vec{q})\,\widetilde{T}(\vec{q}) \\ \Psi_i(\vec{x}) &= \int \widetilde{\Psi}_o(\vec{q})\,\widetilde{T}(\vec{q})e^{2\pi\imath\vec{q}\cdot\vec{x}}\mathrm{d}\vec{q}\end{aligned}$$

HRSTEM

Incoherent image formation process with coherent or partially coherent probe.

STEM ($\widetilde{OTF}(\vec{q}) = \widetilde{T}(\vec{q}) \otimes \widetilde{T}(-\vec{q})$: Optical Transfer Function):

$$
\begin{array}{lll}
I(\vec{x}) & = \langle \Psi_i(\vec{x};t)\Psi_i^*(\vec{x};t)\rangle & \text{(time average)} \\
\Psi_i(\vec{x};t) & = \Psi_o(\vec{x};t) \otimes T(\vec{x}) & (T(\vec{x}) : \text{PSF independent of t}) \\
I(\vec{x}) & = \langle [\Psi_o(\vec{x};t) \otimes T(\vec{x})][\Psi_o^*(\vec{x};t) \otimes T^*(\vec{x})]\rangle & (\otimes \text{ convolution.}) \\
I(\vec{x}) & = [T(\vec{x})T^*(\vec{x})] \otimes \langle \Psi_o(\vec{x};t)\Psi_o^*(\vec{x};t)\rangle & (T(\vec{x}) \text{ is time independent.}) \\
\langle \Psi_o(\vec{x};t)\Psi_o^*(\vec{x};t)\rangle & = |\Psi_o(\vec{x})|^2 & \text{(complete spatial incoherence)} \\
I(\vec{x}) & = |\Psi_o(\vec{x})|^2 \otimes [T(\vec{x})T^*(\vec{x})] & \\
I(\vec{x}) & = I_o(\vec{x}) \otimes [T(\vec{x})T^*(\vec{x})] = I_o(\vec{x}) \otimes P(\vec{x}) & \text{(P: probe intensity)}
\end{array}
$$

Probe function $P(\vec{x})$: source intensity distribution as measured at the sample plane.

Convolution, cross-correlation & autocorrelation

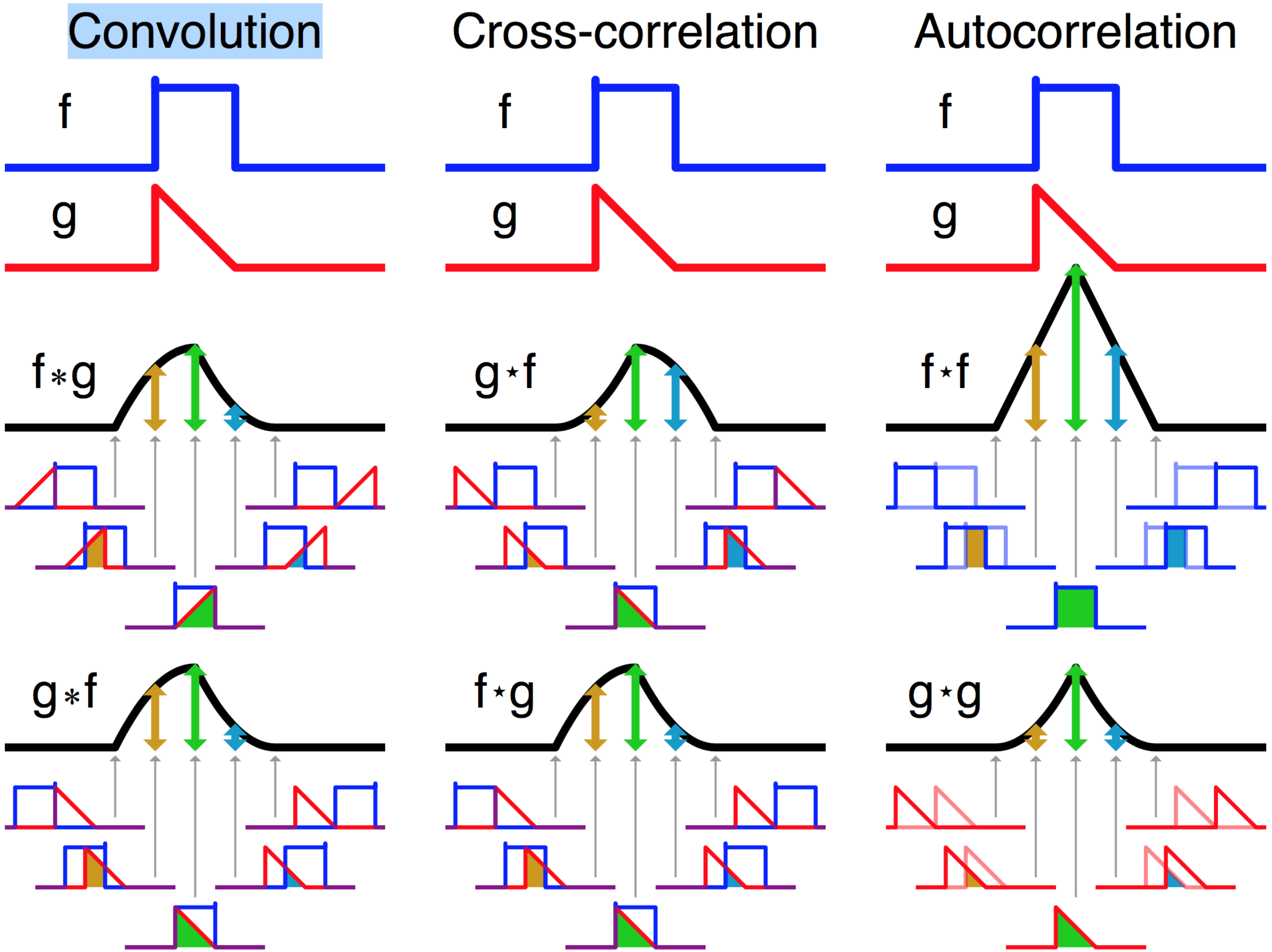

HRTEM / HRSTEM problem: aberrations of optical system

Reaching 0.05 nm resolution sets very strong conditions on aberrations correction.

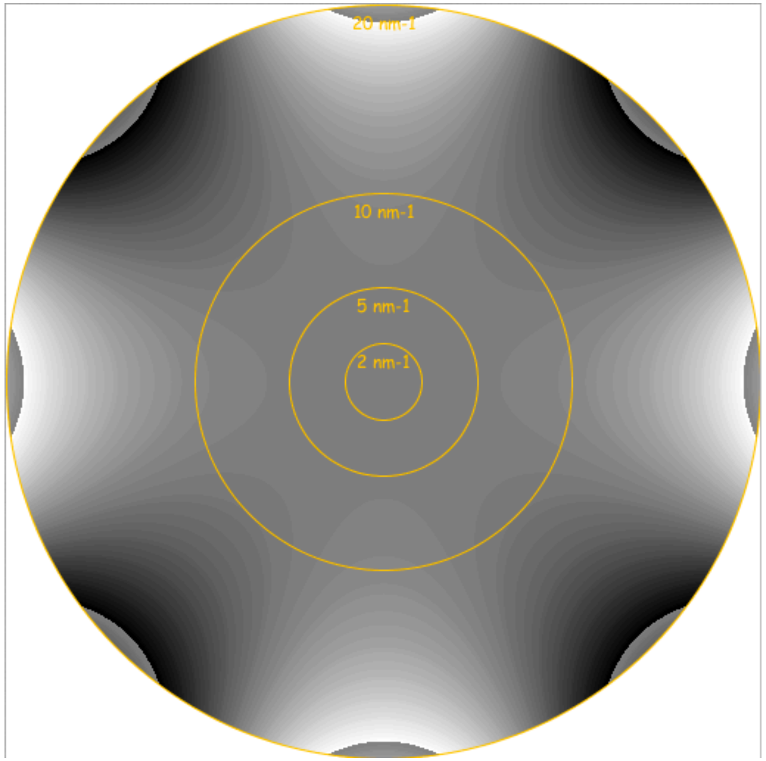

Aberration figure of $C_{34}(0.5\mu\mathrm{m})$, phase jump at $\frac{\pi}{4}$.

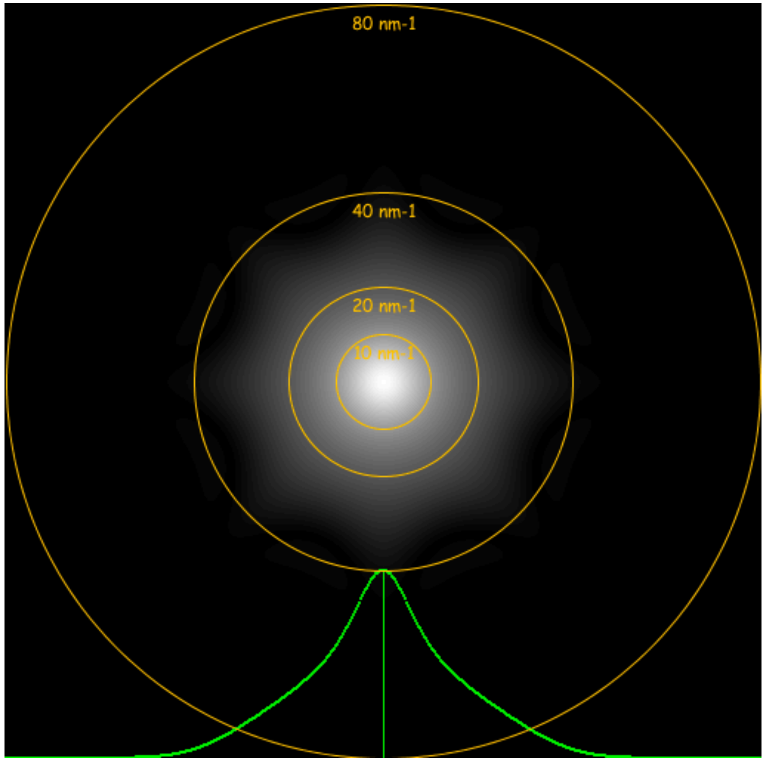

Optical Transfer Function.

Notice that Optical Transfer Function (HRSTEM) transfers higher spatial frequencies than Coherent Transfer Function (HRTEM). OTF is the autocorrelation of the PSF wi itself. Autocorrelation doubles the domain of the function $\longrightarrow$ the $OTF(\vec{q})$ domain is twice as large as the $TF(\vec{q})$.

$P(\vec{x})$: source intensity distribution as measured at the sample plane

Aberrations modify the source intensity distribution. STEM scans the corrected probe $P(\vec{x})$ on the crystal entrance plane ($I(\vec{x}) = I_o(\vec{x}) \otimes P(\vec{x})$).

2 fold astigmatism. 3 fold astigmatism.

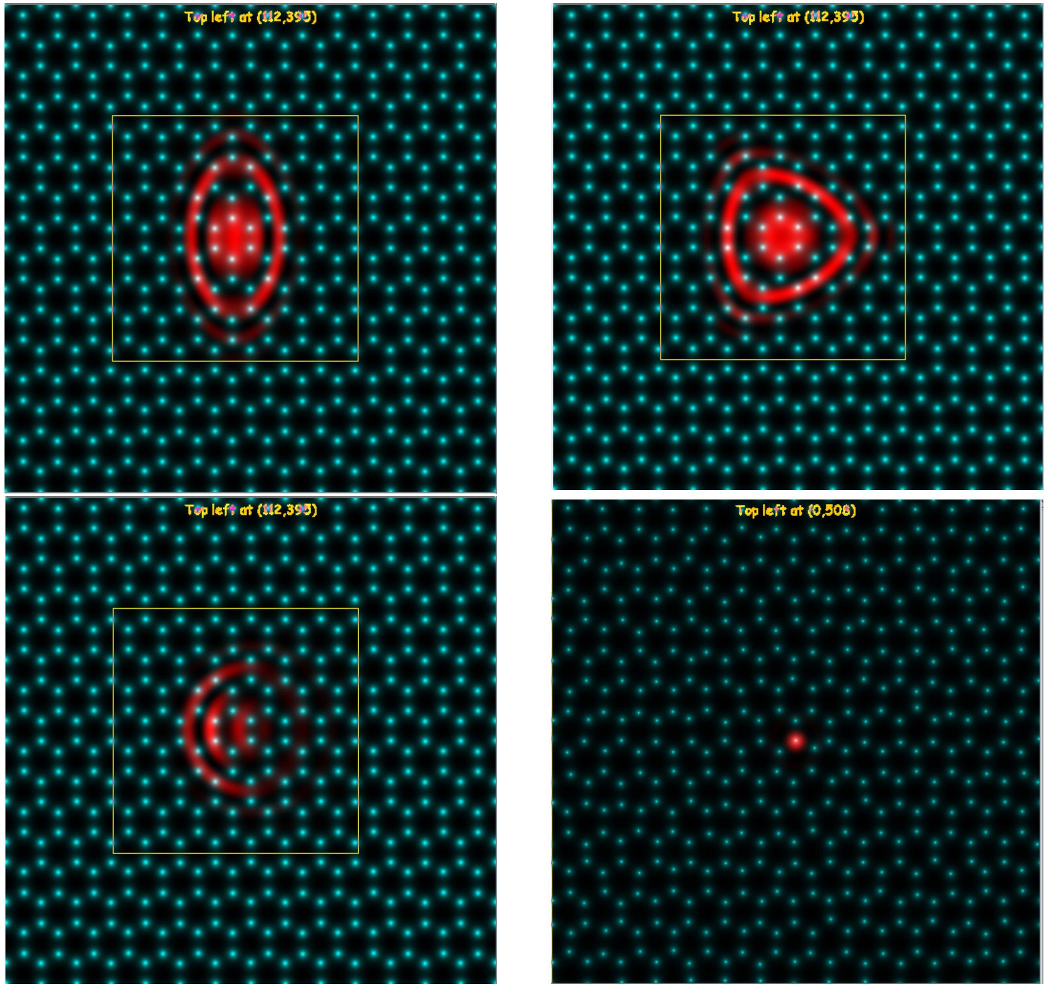

Coma. Corrected probe.

STEM imaging: calculating $I_0(\vec{x})$

Numerous approximations are involved in calculating $I_0(\vec{x})$ (object intensity):

- Simple **projected potential**: no channeling effect (Weak Object Approximation).
- **Multislice** or **Bloch-wave** calculation: channeling + inelastic scattering (absorption or optical potential).
- **Frozen lattice** (phonon) approximation: atoms of super-cell displaced out of equilibrium position, probe scanned on imaged area, intensity collected by annular detector. Allows to simulate HAADF (High Angle Annular Dark Field), BF (Bright Field), MAADF (Medium Angle Annular Dark Field), DPC (Differential Phase Contrast), ...
- References: Allen, Ishizuka, Nellist, Pennycook, Rosenauer, van Dyck, Wang.

Except the first 2 methods, usually rather long simulation time (faster calculations using GPU).

STEM imaging: graphene

Proj. pot. approx. Channeling calc.

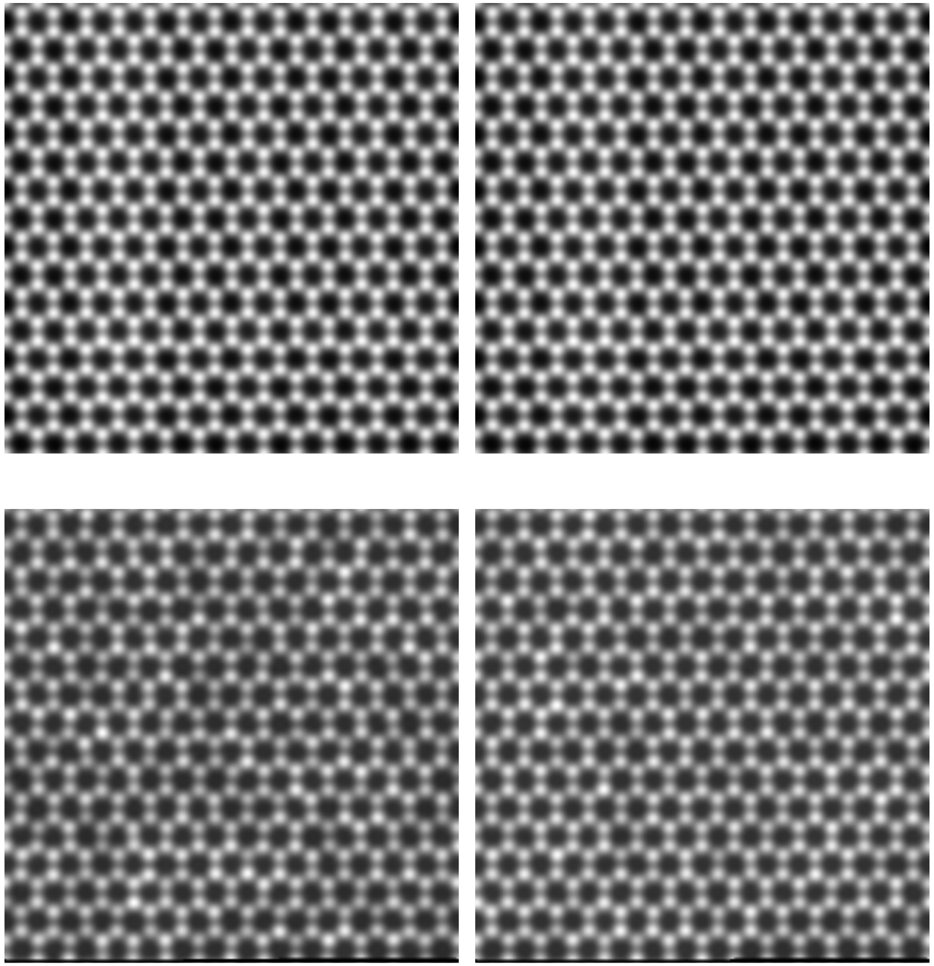

Frozen lattice 5 conf. Frozen lattice 10 conf.

Frozen lattice: sampling is critical and it is necessary to repeat the calculation (10 to 40 times) to image most of the possible atomic configurations.

- Dynamical calculations: how good?
- Optical system.
- Aberrations.
- HRTEM transfer function & HRSTEM: optical transfer function.
- $\longrightarrow$**Comparison HRTEM - HRSTEM**.

HRSTEM - HRTEM comparison: graphene with add atoms

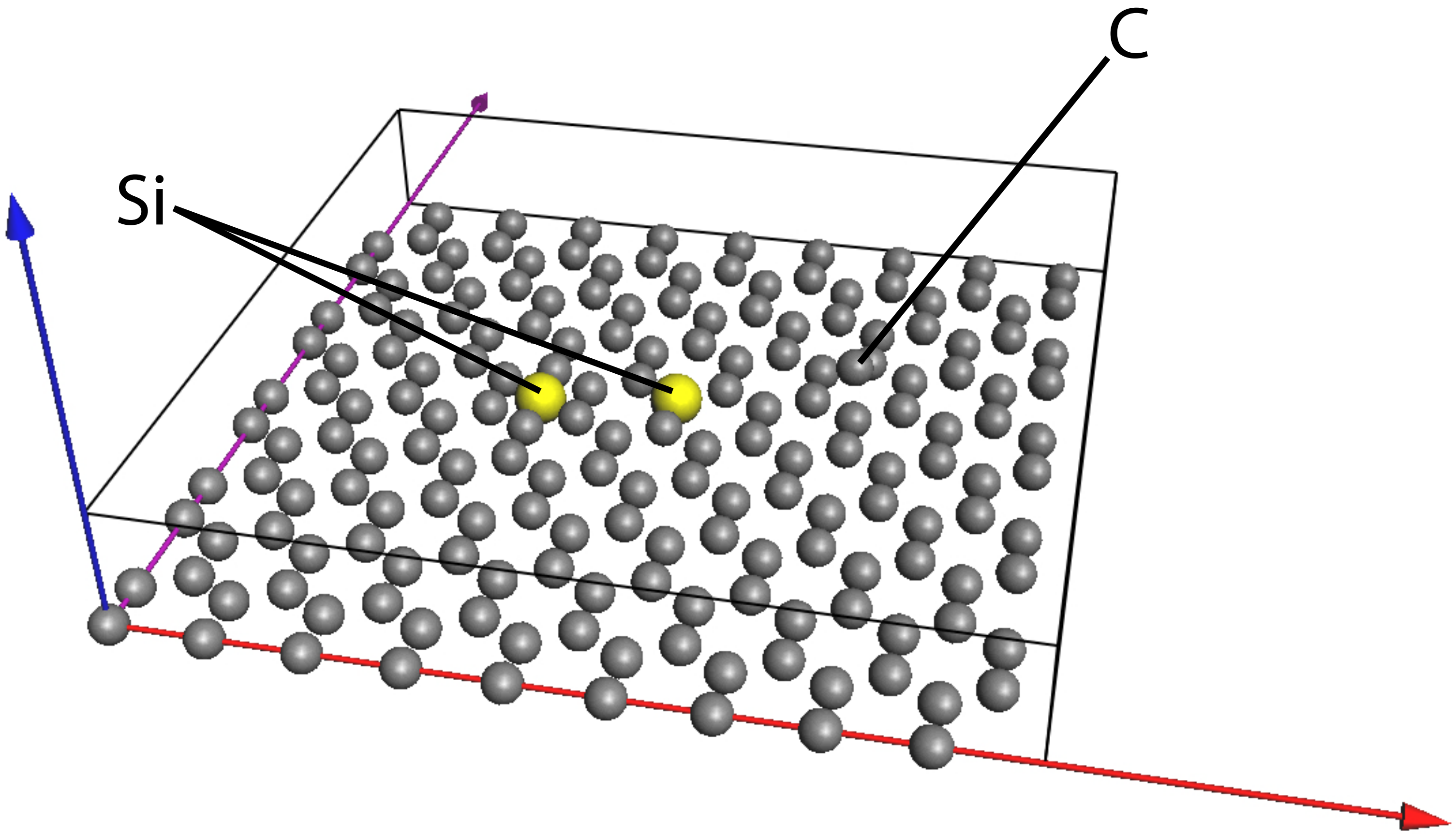

Graphene with Si in 6 C ring, Si substitutional and 2 C column.

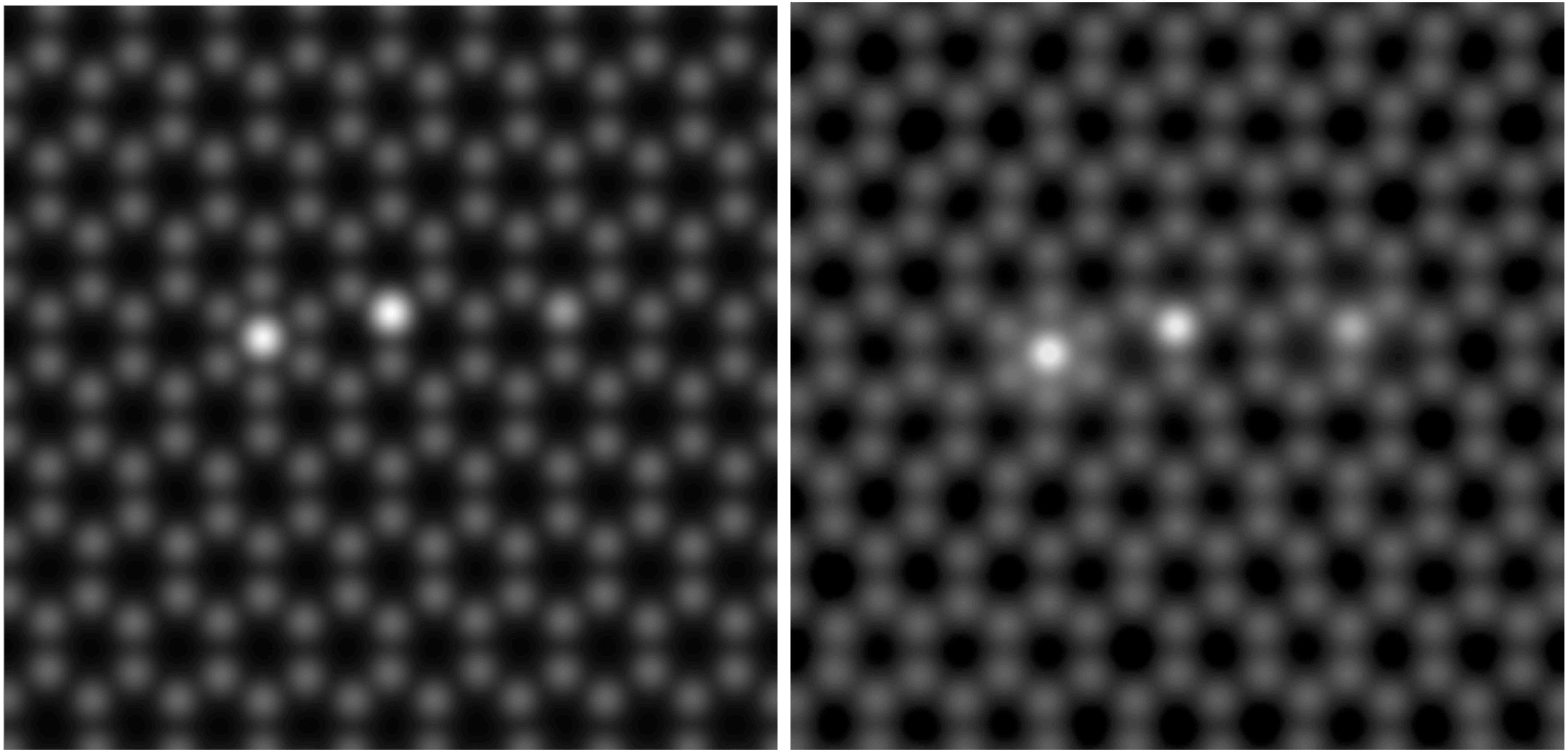

Frozen lattice ($\sim$400 s). Channeling ($\sim$2 s).

One Si shows more contrast than 2 C atoms (i $\sim Z^2$) : 14^2 compared to $\sim 2 \times 6^2$.

Graphene: HRTEM (100 kV, $C_s - 0.033mm$)

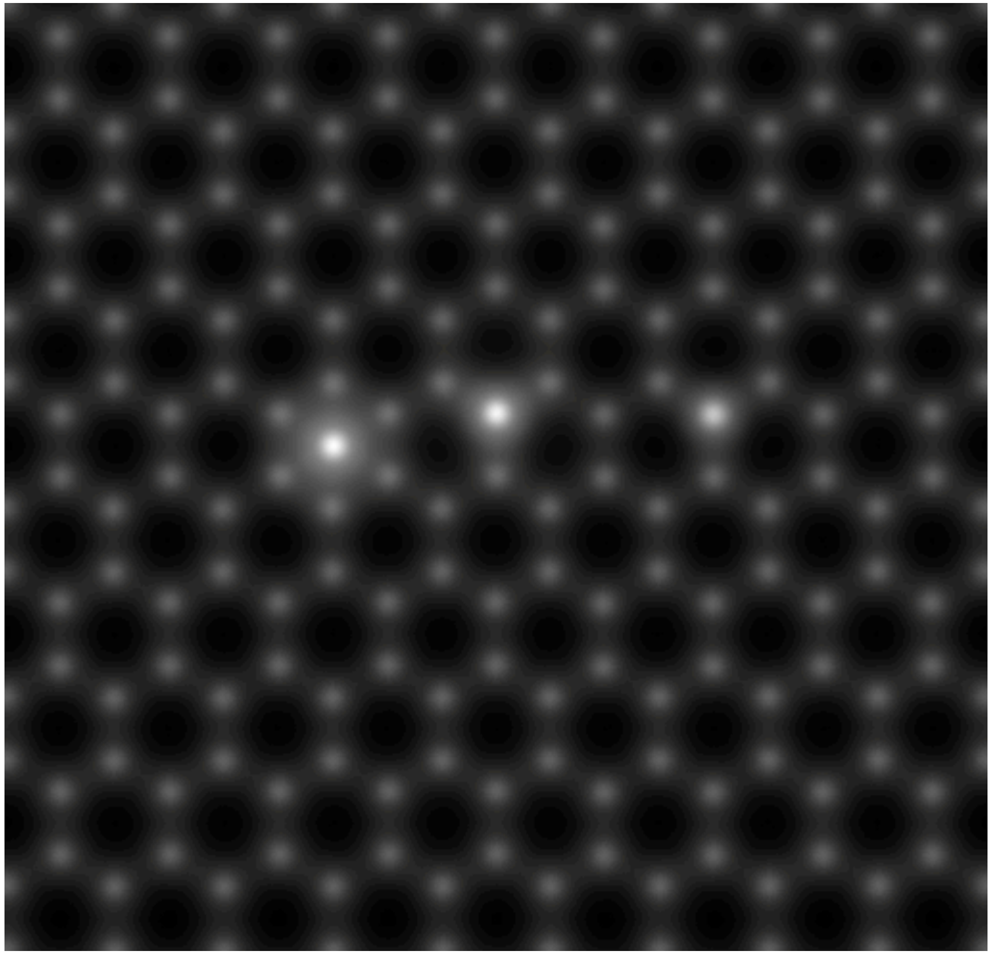

Weak phase object app., $C_c = 0.5mm$

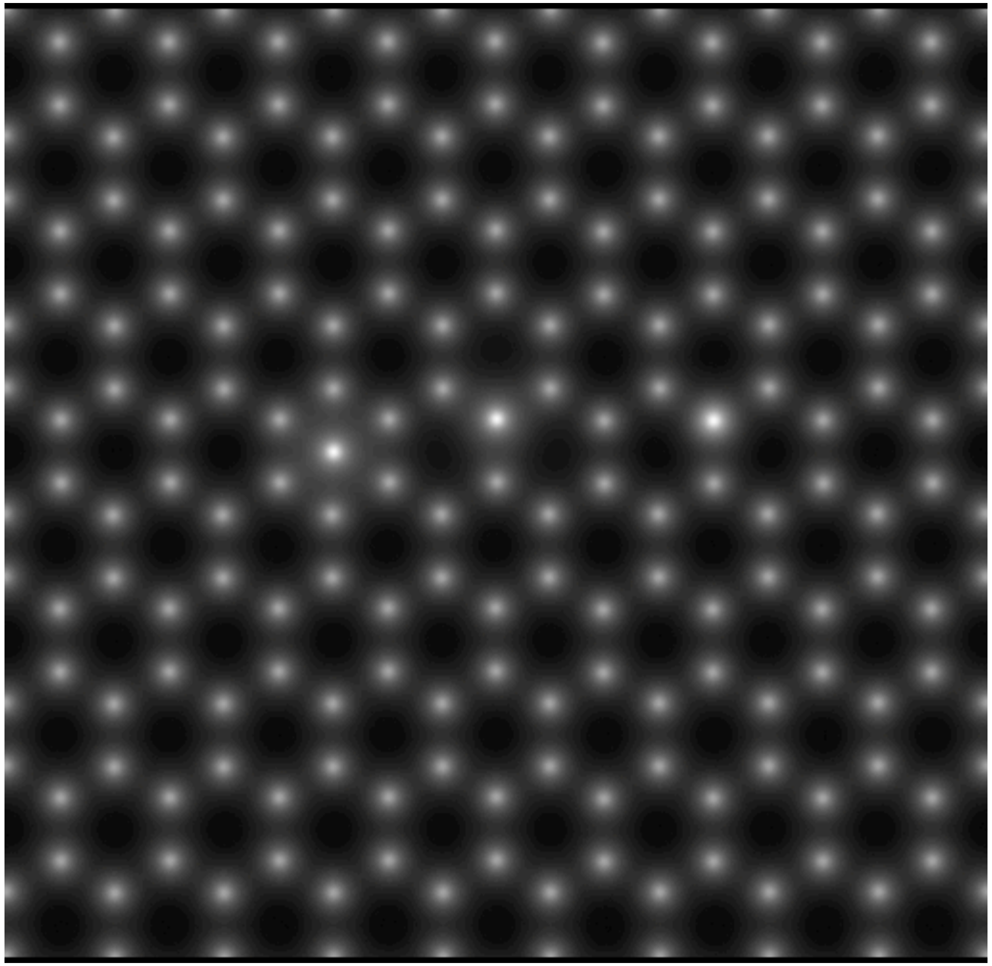

Multislice, $C_s = -0.033mm$, $C_c = 0$, no thermal magnetic noise.

HRTEM does not display the strong contrast difference between one Si and two C as given by HAADF STEM imaging.

HRTEM & HRSTEM image simulations share many calculation methods. Both require precise dynamical calculations that take into account elastic and inelastic electron scattering.

Important difference to remember:

- HRTEM: the wave-function $\widetilde{W}(\vec{q})$ in the image plane is the product of the object wave-function $\widetilde{O}(\vec{q})$ with the transfer function of the microscope $\widetilde{T}(\vec{q})$:

$$\widetilde{W}(\vec{q}) = \widetilde{O}(\vec{q}) \times \widetilde{T}(\vec{q})$$

- HRSTEM: image intensity $I(\vec{x})$ at the detector position is the convolution of the object intensity $I_o(\vec{x})$ with the probe intensity $P(\vec{x})$:

$$I(\vec{x}) = I_o(\vec{x}) \otimes P(\vec{x})$$

As a result we can expect a better spatial resolution and no phasing difficulties using HRSTEM.

Thanks for your attention!